THE ASTROPHYSICAL JOURNAL, 460:L57–L60, 1996 March 20

HERBIG-HARO JETS, CO FLOWS, AND CO BULLETS: THE CASE OF HH 111

J. CERNICHARO[1] AND BO REIPURTH[2]
Received 1995 November 3; accepted 1995 December 19

ABSTRACT

We have carried out high spatial resolution, 12″, CO $J = 2$–1 observations at the IRAM 30 m telescope of the molecular outflow in the HH 111 jet complex. The Herbig-Haro jet is found to coincide with a highly collimated CO flow, with two distinct velocities, possibly providing kinematic evidence that the CO flow surrounds the HH jet. A second well-defined bipolar molecular flow, at large angles to the principal flow axis, coincides with the HH 121 infrared flow that emanates from the (presumably binary) VLA driving source; the region thus harbors one of the rare quadrupolar molecular flows. Extremely high velocity CO is found toward the principal HH working surface at the same velocity as the optically emitting gas, whereas this emission is weak toward the Herbig-Haro jet. Since the inclination of the HH jet is known from optical observations to be 10° to the plane of the sky, we conclude that there is CO in the flow with space velocities of up to 500 km s^{-1}! Further out, and precisely along the flow axis, we have discovered three equidistant CO bullets with space velocities of about 240 km s^{-1}, which are not detected in the optical. We interpret these bullets as the result of earlier eruptions from the energy source that are now moving through an ambient medium so tenuous that no observable shock interaction takes place. Finally, we discuss the physical relation between the Herbig-Haro jet, the CO bullets, and the low-velocity molecular outflow. We favor the view that HH jets and CO bullets, which represent different manifestations of the same physical phenomena, are driving the low-velocity molecular outflow.

Subject headings: ISM: individual (HH 111) — ISM: jets and outflows — ISM: molecules — stars: formation — stars: mass loss

1. INTRODUCTION

The deeply embedded stars driving Herbig-Haro (HH) flows are among the youngest stars known. The supersonic shocked jets that emanate from these stars testify to the current release of large amounts of energy in or near the nascent stars. Molecular outflows are another mass-loss driven phenomenon taking place during the earliest evolutionary stages. They are much more massive and normally less well collimated than the HH flows, but as argued by Raga (1991), the two types of flows may carry the same order of momentum. An important unsettled question concerns the relationship that HH flows and molecular outflows hold to one another. One attractive possibility is that HH jets, in their episodic outbursts, transfer enough momentum to drive the molecular outflows; some observational evidence has been found to this effect (see, e.g., Chernin & Masson 1991; Olberg, Reipurth, & Booth 1992; Heathcote & Reipurth 1992), and theoretical mechanisms for the transfer of momentum from the jet to its ambient medium have been proposed (see, e.g., Raga & Cabrit 1993; Masson & Chernin 1993).

One of the finest HH jets known to date is HH 111 in L1617 in the Orion B cloud complex (Reipurth 1989). The whole jet complex stretches over 367″, which at the presumed distance of 460 pc corresponds to 0.82 pc. It consists of a bright highly collimated jet, a small faint counterjet, and at least four bow shocks, two on each side of the source. Proper motions are large, between 300 and 600 km s^{-1}, and directed away from the driving source, IRAS 0591+0247, which is a deeply embedded 25 $L_\odot$ class I source (Reipurth, Raga, & Heathcote 1992). The source was recently detected at 2.0 and 3.6 cm at the VLA (Rodriguez & Reipurth 1994). The HH flow lies almost in the plane of the sky, with an inclination of only 10°, with the western lobe approaching us, and the eastern one receding from us. The energy source of HH 111 is embedded in a 30 $M_\odot$ cloud core. Along the axis of the HH complex, a major molecular outflow has been detected. The red (eastern) lobe has an extension of 0.7 pc, which is twice as large as the blue lobe. This difference probably originates because the blue lobe moves into almost empty space, whereas the red lobe ploughs along the southern edge of the L1617 cloud (Reipurth & Olberg 1991).

In this Letter, we present detailed observations of the inner lobes of the molecular outflow, demonstrate the presence of a highly collimated molecular jet, and discuss constraints on models of jet-driven molecular outflows. We have also discovered several CO bullets further out along the blue flow axis, and we discuss their nature and relation to jet bow shocks.

2. OBSERVATIONS

CO data for the high-velocity gas were obtained in 1990, 1992, and 1994 with the 30 m IRAM radio telescope. Three SIS receivers at 3, 2, and 1 mm were used simultaneously with receiver temperatures of 100, 100, and 150 K, respectively. The spectrometers were two 512×1 MHz filter banks, one 256×100 KHz filter bank, and an autocorrelator with 2048 channels and spectral resolution of 37 KHz. The weather was excellent during all observing runs, with typical zenith opacities of 0.05–0.1 and of 0.3 at 230 and 115 GHz, respectively. For the mapping of the region covered by the HH flow (a region of $240'' \times 120''$ centered on the VLA source) the observing procedure consisted in a series of fast raster maps (1 hr each) followed by a pointing check. The sampling spacing was 7″, and the integration time per point was 30 s. Each raster was repeated until a signal-to-noise ratio of 10 was reached in the velocity range from −5 to +12 km s^{-1}. Figure 1 shows the

[1] Observatorio Astronómico Nacional, Campus Universitario, Apartado 1143, E-28800 Alcalá de Henares (Madrid), Spain.
[2] European Southern Observatory, Casilla 19001, Santiago 19, Chile.

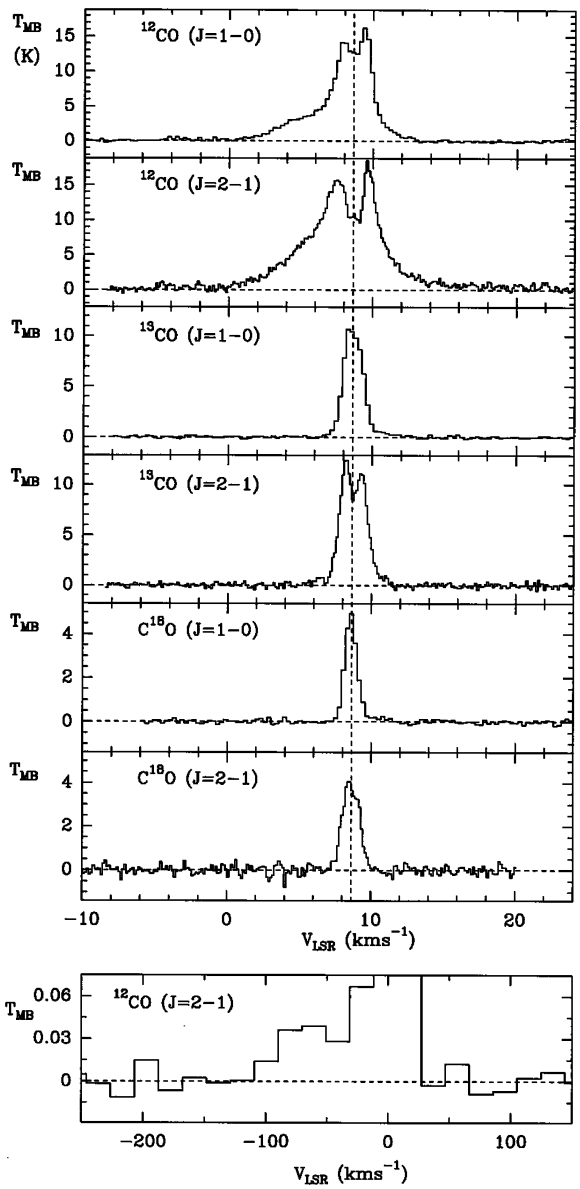

FIG. 1.—Observed $J = 1–0$ and $J = 2–1$ spectra of CO, ^{13}CO, and C^{18}O toward the VLA source of the HH 111/HH 121 system. The two velocity components detected in the $J = 2–1$ line for all the isotopes corresponds probably to the interaction of the molecular jet with the ambient gas (see text). The bottom spectrum corresponds to the average emission in the inner jet between the VLA source and 60″ west.

$J = 1–0$ and $J = 2–1$ lines of the different CO isotopes toward the central position and the CO $J = 2–1$ emission averaged over the inner part of the HH jet. The resulting morphology of the blue and red CO $J = 2–1$ integrated intensity is shown in Figure 2 (Plate L6). The CO emission for selected velocity intervals is shown in Figure 3 (Plate L7), while Figure 4 (Plate L8) shows a velocity-position strip along the direction traced by the optical jet. During the completion of this strip we detected high-velocity CO gas right at positions where the optical activity disappeared. A region 250″ long and 48″ wide starting 80″ west of the central VLA source was mapped using the wobbler switching method along the jet axis at a P.A. of 277°. The integration time per point was 5 minutes with a wobbler throw of 240″ in azimuth. Molecular gas at velocities as high as -80 km s^{-1} can be observed between 80″ and 330″ west of the VLA source. Figure 5 (Plate L9) shows the emission of the CO $J = 2–1$ line in four selected velocity ranges, and Figure 6 (Plate L10) shows a velocity-position diagram of the CO emission similar to that of Figure 4 but with a much larger velocity and position coverage.

3. THE MOLECULAR JETS: A QUADRUPOLAR SYSTEM

The short blue lobe found by Reipurth & Olberg (1991) is seen in our higher resolution CO $J = 2–1$ data (see Fig. 2) to be a highly collimated molecular jet about 90″ long with a collimation factor of about 9. The red lobe is shorter, but precisely aligned along the axis of the blue lobe. The blue lobe ends at the location of the bow shock *P* and the optical knots *Q*, *R*, *S* (see Reipurth 1989). The velocity dispersion of the CO gas is largest at the head of the molecular jet, just as expected for a bow shock (from -10 to $+7.5$ km s^{-1}). The CO blue lobe is shorter than the HH lobe, in which the most distant bow shock *V* is located almost 150″ from the VLA source. Although the quiescent gas of the globule has an extent reaching as far west as the tip of the molecular outflow, at these larger distances it has a low visual extinction ($A_V \leq 2$ mag) and a low volume density [$n(H_2) \approx$ a few 10^2 cm^{-3}] as derived from our molecular data. Indeed, the deep CCD images of Reipurth et al. (1992) show that the globule has a rather well-defined surface only about 20″ from the VLA source, beyond which the visual extinction and the amount of molecular gas are very low. Consequently, the HH jet is emerging into a low-density medium, and therefore the molecular outflow must either be material dragged along from inside the globule or must have been swept up from the thin ambient medium and compressed, but we consider this latter possibility very unlikely.

As shown in the infrared images of Gredel & Reipurth (1993, 1994) there is a second bipolar jet, HH 121, emanating from the VLA source at large angles to the HH flow. This flow is very pronounced in Figure 2. The blue part of the jet is particularly apparent and runs northeast from the VLA source, while the red lobe to the southwest is weaker and shifted slightly eastward of the HH knots, perhaps because of a density-gradient in the surrounding cloud. In Figure 3 the quadrupole flow is particularly apparent. The gas associated with the blue lobe of HH 121 appears at LSR velocities between $+2$ and $+3$ km s^{-1}, while its red counterpart corresponds to velocities larger than $+9$ km s^{-1}.

The velocity maps of Figure 3 show a pronounced case of the well-known acceleration effect for the HH 111 CO blue lobe, seen also in a number of other molecular outflows, e.g., the NGC 2024 FIR 5 flow (Richer, Hills, & Padman 1992). The peak intensity of each of the velocity intervals moves closer to the source as the velocity decreases, until the peak is centered on the VLA source just before the flow blends with the ambient cloud.

Although the blue and red integrated intensity maps shown in Figure 2 seem to indicate a rather smooth appearance for the HH 111 molecular jet, the velocity interval maps of Figure 3 and the velocity-position diagram of Figure 4 reveal that there are several clumps in the outflow. In particular, the spatial distribution of the gas at velocities between $+4$ and $+6$ km s^{-1} and at distances larger than 20″ west seem to delineate the walls of an expanding cavity or tube surrounding the optical jet similar to that found in HH 1–2 by Martín-Pintado & Cernicharo (1987) and in HH 34 by Cernicharo (1991). The

PLATE L6

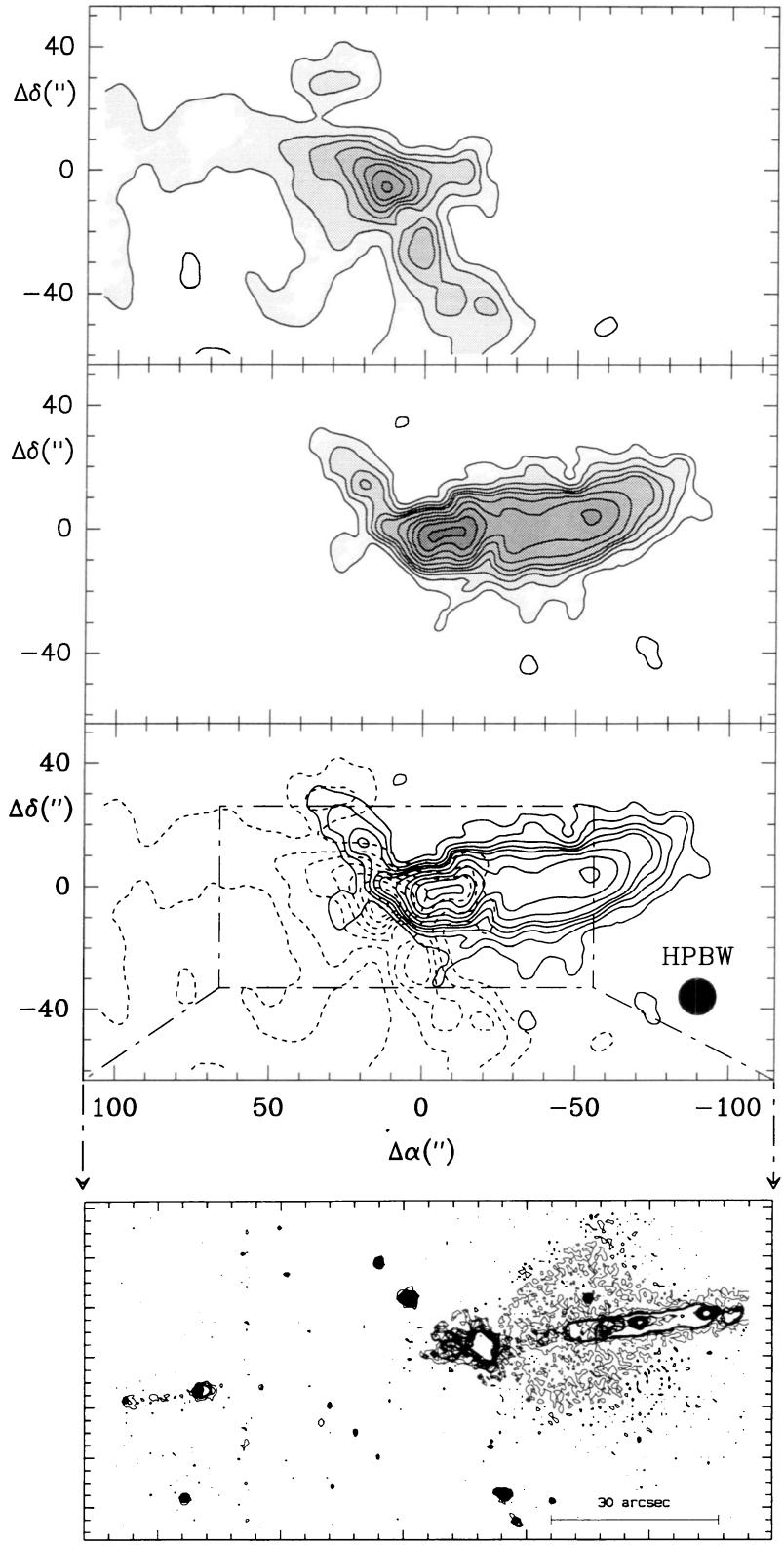

FIG. 2.—Two upper panels show integrated CO intensity for velocities between −5 and +7 km s^{-1} and between +10.5 and +15 km s^{-1}, respectively. The central position corresponds to the VLA source ($\alpha_{1950} = 05^h49^m9\overset{s}{.}3$, $\delta_{1950} = 2°\ 47'\ 48''$). The beamwidth is 12″, and the spacing of the data over the full region is 7″. The third panel combines the blue- and redshifted lobes and indicates with a box the location of the optical/infrared composite of the HH 111 complex seen in the lowest panel (from Gredel & Reipurth 1994). The first contour and step are 1 K km s^{-1}.

CERNICHARO & REIPURTH (see 460, L58)

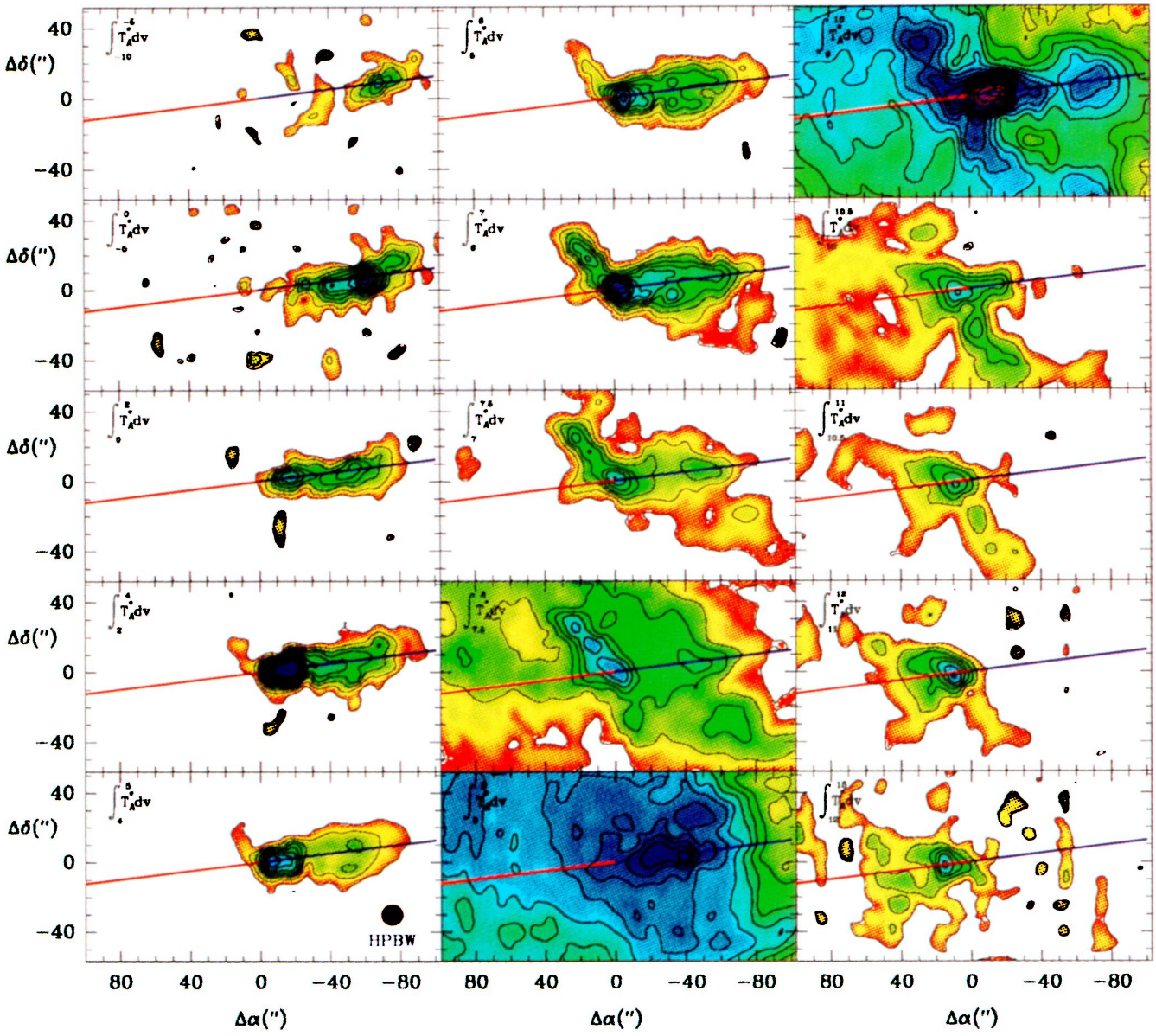

FIG. 3.—Integrated CO intensity for the velocity intervals indicated at the top left of each panel. The thick line crossing the different panels indicates the axis of the HH flow (the red/blue color of this line corresponds to the gas having positive/negative velocity). The first feature that appears in this figure is the long molecular jet coinciding with the HH flow; see panels corresponding to velocities lower than +2 km s^{-1}. At velocities between +5 and +7.5 km s^{-1} a second jet is clearly visible running from the VLA source toward the northeast. This jet has its red counterpart running from the VLA source toward the southwest at velocities between +10 and +12 km s^{-1}. The red counterpart of the main blue molecular jet also appears at these velocities, but it is much less collimated and is oriented in the direction traced by the optical jet. The ambient gas appears at velocities between +7.5 and +10 km s^{-1}. The first contour and step are 0.7 and 0.8 K km s^{-1}, respectively, for panels corresponding to velocities lower than 7.5 km s^{-1}; for velocities larger than 10 km s^{-1} they are 0.4 and 0.8 K km s^{-1}, respectively; between 7.5 and 10 km s^{-1} the first contour and step are 8 and 1.5 K km s^{-1}, respectively.

CERNICHARO & REIPURTH (see 460, L58)

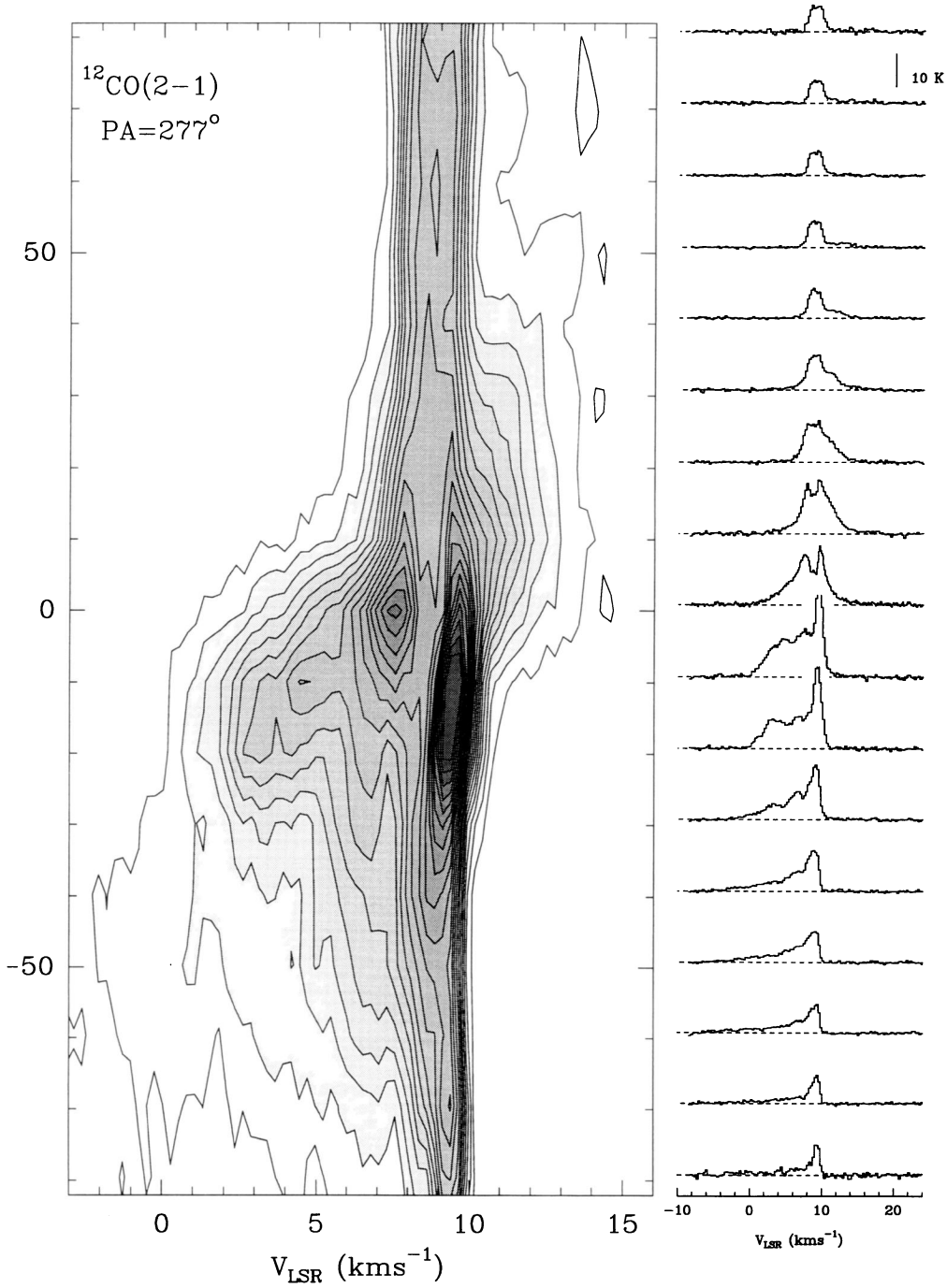

FIG. 4.—Velocity-position diagram for the emission of CO along the jet direction in the inner HH 111 flow. Spectra are shown at positions separated each by 10″. The first contour and step in the diagram are 1 K. Note that the red emission is less extended than the blue one. The blue lobe has several velocity components which could be associated to an expanding cavity (see text).

CERNICHARO & REIPURTH (see 460, L58)

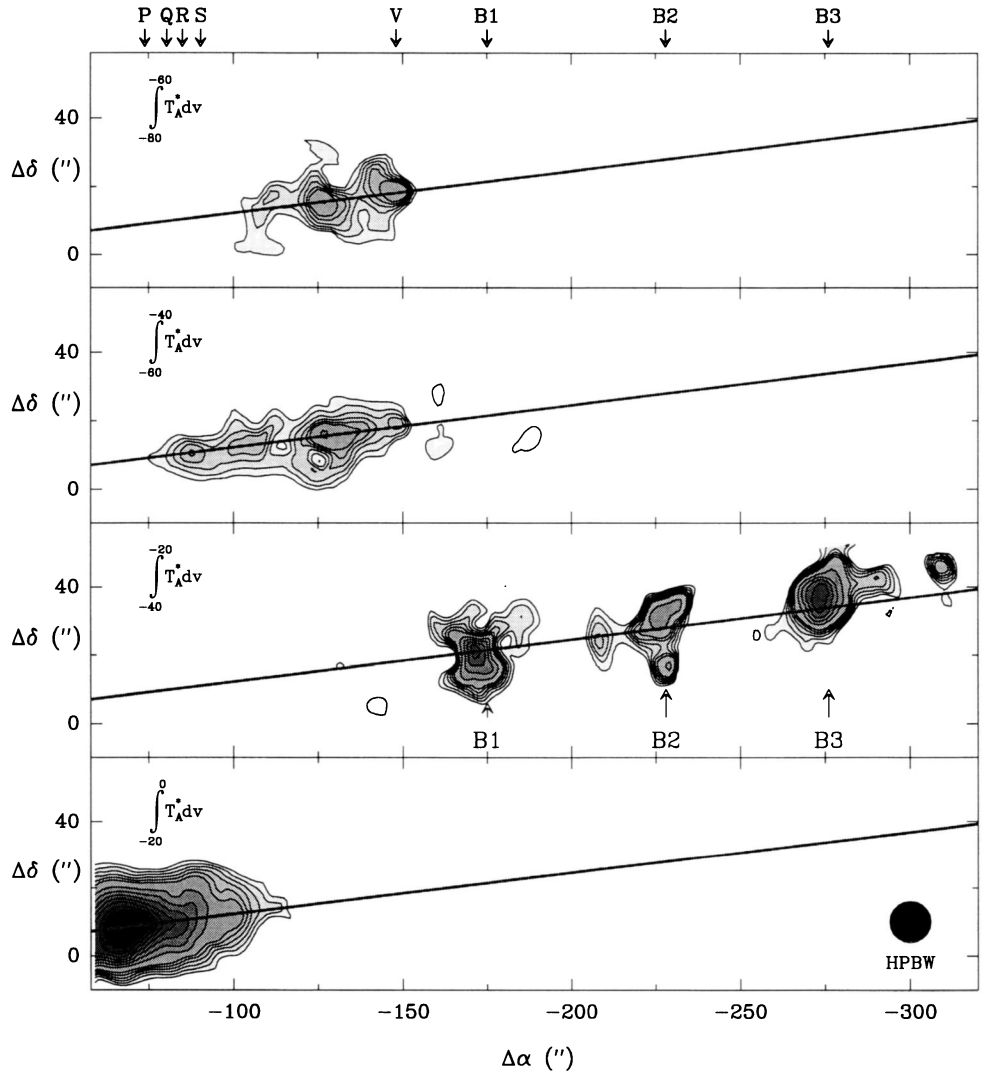

FIG. 5.—CO $J = 2$–1 integrated intensity at velocities between -10 and -80 km s^{-1}. Note that high-velocity gas appears just when the low-velocity gas disappears (*bottom panel*). The three objects regularly spaced in the second panel from the bottom correspond to the three bullets discussed in the text. Contours are 0.6–2.2 by 0.3 K km s^{-1} and 3–10 by 0.8 K km s^{-1}. The map was made along the jet axis at a P.A. of 277°.

CERNICHARO & REIPURTH (see 460, L58)

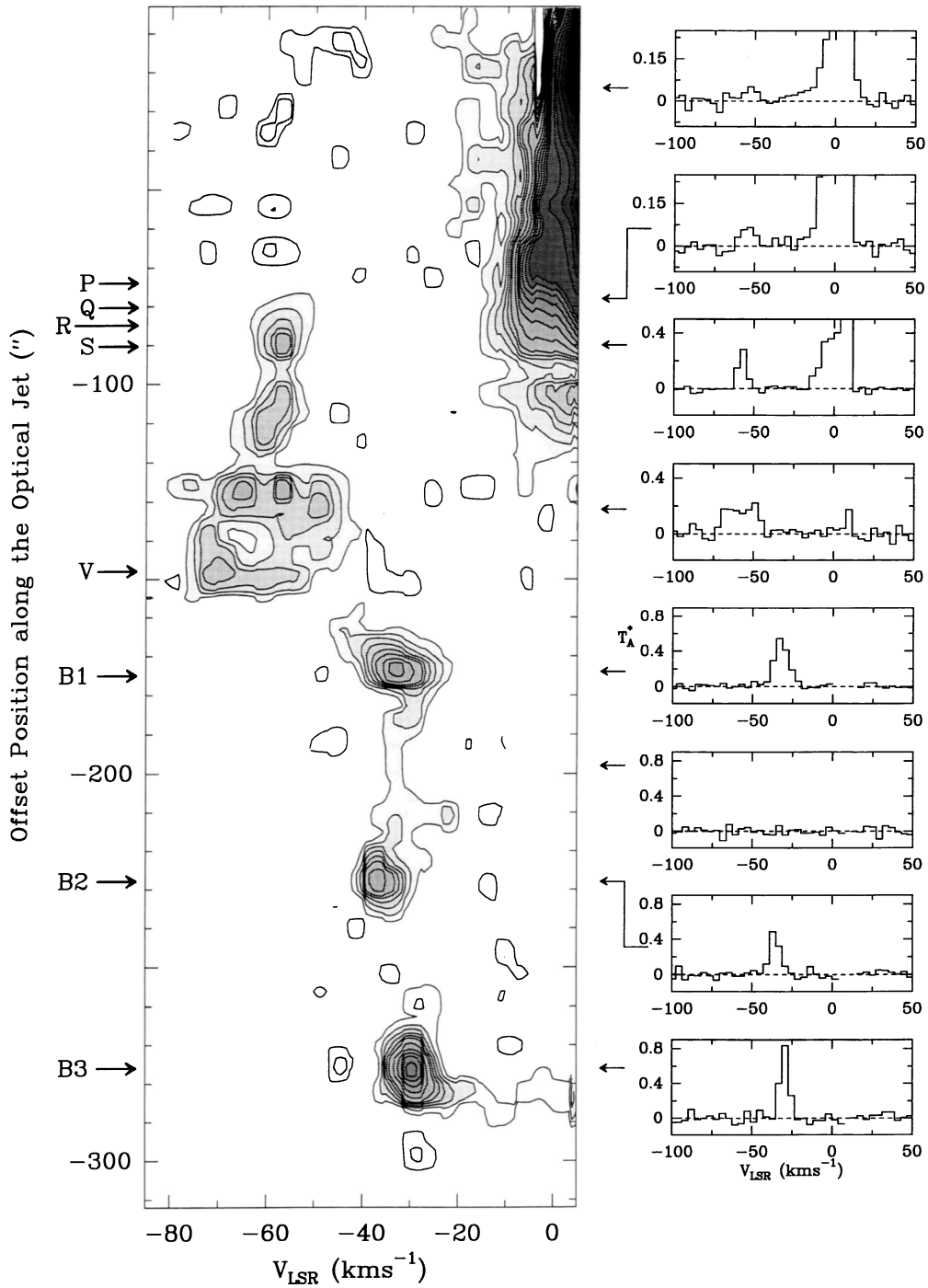

FIG. 6.—Velocity-position diagram for the high-velocity CO gas. Spectra at selected positions are also shown. Note that the data used here correspond to the 1 MHz filters while the diagram of the inner flow in Fig. 4 corresponds to high spectral resolution data (with less velocity coverage). The different bullets are clearly visible and are labeled B1–B3 for the neutral gas unassociated with optical knots. The position of the optical knots are indicated by crosses and labeled *P*, *Q*, *R*, *S*, and *V* (Reipurth 1989). Contours are 0.05–0.3 by 0.05 K, 0.4–1 by 0.1 K, and 1.5–10 by 0.5 K.

CERNICHARO & REIPURTH (see 460, L58)

front and the rear of such a cavity could be traced by the gas at velocities between +7 and +10 km s^{-1} (rear) and between 0 and +4 km s^{-1} (front; see also the models by Cabrit & Bertout 1990). The same spatial structure, i.e., an expanding tube or cavity, could also fit the kinematics of the gas near the VLA source as indicated in Figures 3 and 4. The absorption dip observed in the CO lines toward the central position (see also Fig. 1) is clearly visible in Figure 4 and appears only around the central source. Although it could be interpreted as self-absorption, the velocity component at +9.7 km s^{-1} is detected over the full extent of the blue molecular jet and could correspond to a redshifted perturbation of the ambient cloud by the bipolar outflow. The blue counterpart of this perturbation is also visible in the same region but unfortunately the ambient gas at +9 km s^{-1} renders very difficult the interpretation of the data.

4. THE HIGH VELOCITY BULLETS

The gas associated with the molecular flows in HH 111/HH 121 appears at velocities between −10 and +15 km s^{-1}. This gas covers the region delineated by the optical jet. However, just beyond bow shock *P* and optical knots *Q*, *R*, and *S* (see Reipurth 1989), where we expected no more outflow emission, we did find strong CO emission at extremely high velocity (EHV). Figure 5 shows the integrated CO emission in four high-velocity intervals. Beyond the optical bow shock *P*, which is at position 75″ from the VLA source, the CO emission appears at velocities between −40 and −80 km s^{-1}. Assuming an angle of 10° to the plane of the sky for the HH 111 complex as derived from radial velocity and proper motion measurements of the HH jet (Reipurth et al. 1992), the true space velocity of the high-velocity CO emission is between 250 and 500 km s^{-1}! This gas is detected extending from 80″ to 150″ west of the VLA source. The first EHV CO emission appears just after knot *P* at a LSR velocity of −60 km s^{-1}, which is identical to the LSR velocity of the ionized gas in this knot (Reipurth 1989). The EHV CO emission consists of four bullets at positions 80″ (knot *P*), 110″, 125″, and 150″ (knot *V*) west (see Figs. 5 and 6). Figure 6 shows a velocity-position diagram of the CO emission along the direction of the optical jet together with some selected CO spectra. Important variations in the line shape and intensity are observed from the first CO bullet at 80″ west to the last one at 150″ west (optical knot *V*). Like for the low-velocity gas at these positions, the velocity dispersion in the EHV bullets is very large, as could be expected from the interaction of the EHV with the ambient gas. The EHV CO gas disappears beyond knot *V*. This knot has an LSR velocity of −70 km s^{-1} (Reipurth 1989), which is also identical to the velocity of the neutral gas at this position.

Between the VLA source and bow shock *P* the EHV CO emission is very weak. We have obtained an average CO spectrum for the inner part of the HH jet by averaging all the data between the VLA source and position 60″ west along the jet. The spectrum (see Fig. 1, *bottom panel*) consists of a broad emission feature centered at −70 km s^{-1} (deprojected velocities relative to the ambient cloud as high as 500 km s^{-1}) with an intensity of 30 mK. This weak emission could be associated to the neutral counterpart of the inner HH jet. Assuming a kinetic temperature of 100 K for this gas, a CO abundance of 10^{-4}, a distance of 460 pc, thermalization for the $J = 2$–1 CO line, and the CO/H_2 conversion factor of Cernicharo & Guélin (1987), then the mass of this neutral gas could be as high as 0.0006 $M_\odot$. The associated momentum is ≈0.3 $M_\odot$ km s^{-1} (these numbers have to be taken with caution in view of the large uncertainties involved in their determination).

Beyond the optical bow shock *V*, we have discovered three CO bullets (hereafter referred to as bullets 1, 2, and 3, in order of increasing distance from the source) with separations of ≈55″. We have taken a deep [S II] image of the region with the ESO 3.5 m NTT and found no optical emission associated with these bullets. However, the bullets are perfectly aligned along the direction defined by the optical jet. Bullet 3 appears at 0.63 pc from the VLA source (position 280″ west). Again, for an angle of 10° to the plane of the sky, the deprojected velocity of the three bullets is about 240 km s^{-1}. This velocity implies an episodic ejection of matter every ≈500 yr. The outermost bullet could be emitted from the central source some 2600 yr ago. Note that the distance between bullet 1 and that associated with the optical bow shock *P* is also about 55″. The bright bow shock *V*, however, is located midway between knot *P* and bullet 1.

From the maps shown in Figure 5 the bullets appear to be barely resolved with the 12″ beam at 230 GHz. However, some of the bullets are clearly elongated in the direction of the jet. Taking into account the different sizes of the $J = 1$–0 and $J = 2$–1 beams, the CO $J = 2$–1/$J = 1$–0 intensity ratio in the three bullets is about 1.6–2.0. In the optically thin case and assuming equal excitation conditions for the $J = 1$–0 and $J = 2$–1 lines, this ratio could correspond to excitation temperatures of about 12–16 K. We could also consider the possibility of moderate optically thick emission ($\tau \approx 1$) in a subthermally excited gas. Unfortunately, no ^{13}CO observations are available and we cannot deduce the opacity of the CO emission. Assuming optically thin emission and $T_{ex} = 15$ K, then the masses of the bullets are a few 10^{-4} solar masses, i.e., similar to that of the bullets in other young low-mass star forming regions (see Bachiller et al. 1990; Bachiller & Cernicharo 1990).

5. HH FLOWS AND MOLECULAR OUTFLOWS

A number of theoretical works have appeared in recent years exploring the possibility that HH jets are driving molecular outflows. Since HH jets are episodic, with dynamical ages of the order of 10^3 yr, the longer lasting molecular outflows would be the time averaged result of the momentum transferred from the many pulses of HH jets passing through their ambient medium.

Models have concentrated on two mechanisms. First, gas can be accelerated by the passage of a working surface of a jet (internal or leading) that "sweeps up" ambient material and then releases it in a turbulent wake identified with a molecular outflow. This has been explored with both analytic (Raga & Cabrit 1993; Masson & Chernin 1993) and numerical techniques (Chernin et al. 1994), and the effect of many pulses was studied by Raga et al. (1993). Second, gas can suffer "lateral entrainment" along the boundary between the jet beam and its environment (Cantó & Raga 1991; Stahler 1994; Raga, Cabrit, & Cantó 1995). The high collimation we observe, with a flow barely resolved in our beam, seems to be more consistent with the first family of models. Note in particular that Raga et al. (1993) find very narrow molecular outflows resulting from the passage of a large number of internal working surfaces that intercept the jet beam and eject material sideways.

Our data present several immediate questions:

What is the nature of the three outermost high-velocity bullets?—The most straightforward explanation is that these bullets are working surfaces, otherwise similar to the ones seen optically closer to the source. Morse et al. (1993) found

evidence that the outer optically visible working surface *V* is moving into a comoving medium, suggesting that it has been preceded by one or more other working surfaces. This supports our interpretation of the bullets as earlier eruptions from the energy source. The regular spacing, unless fortuitous, suggests that the bullets are traveling away from the source at constant speed. With radial velocities relative to the cloud core of about 40 km s^{-1} and assuming the same angle of 10° to the plane of the sky as for the HH jet, we see that the three outermost CO bullets are moving with space velocities of about 240 km s^{-1}. The reason that three of these bullets are not optically visible is most likely that the ambient medium density at these larger distances from the main cloud core is so low that there is no shock interaction between bullets and the near-vacuum through which they move. These bullets, together with those detected over optical knots *P* to *V*, have similar masses and velocities to those found in other low-mass star forming regions like L1448 or HH 7-11 (Bachiller et al 1990; Bachiller & Cernicharo 1990). It is tempting to conclude that not only bullets *P* to *V*, but all CO bullets in HH 111 and in other low-mass star forming regions are associated with bow shocks produced by HH jets. In some cases, lack of dense ambient gas permits the detection of the HH jet in the optical, while in others they remain invisible because they are embedded in large amounts of high extinction material.

Why do we not find strong emission from the high-velocity gas associated with the HH jet?—The CO gas detected toward the jet has velocities of typically up to 10 km s^{-1} relative to the cloud core, much less than the high-velocity gas associated with the optical bow shocks and the bullets. Emission at −70 km s^{-1} is also detected along the jet but at very low levels (about 30 mK; see Fig. 1). The mass associated to this component could be as high as 0.0006 $M_\odot$. One possibility to explain the low CO emission is that the presence of shocks in the HH jet has dissociated the CO in the jet stream. In addition, any CO gas in the body of the jet may have so high a kinetic temperature that the opacity in the $J = 1$–0 and $J = 2$–1 line of CO drops, resulting in the CO emission being weak. In addition, the size of the innermost optical bow shocks is much smaller than those of knots *P*–*V* which are associated to some of our CO bullets. Consequently, beam dilution for the high-velocity gas in the inner regions could also be larger than toward the external bullets, which are hardly resolved with the HPBW of the 30 m telescope. We note that in L1448, which is the prototypical outflow with extremely high-velocity gas (Bachiller et al. 1990), the intensity of the CO bullets also decreases toward the position of the powering engine.

How do mass transport rates of the HH jet and the CO *bullets compare?*—Based on line ratios and shock models, Hartigan, Morse, & Raymond (1996) derive a mass-loss rate of $1.8 \times 10^{-7}\ M_\odot\ yr^{-1}$ for the HH 111 jet. If we take the mass for a bullet to be $2 \times 10^{-4}\ M_\odot$ and adopt the observed interval of passage of 500 yr, we derive a time averaged mass transport rate for the CO bullets of $4 \times 10^{-7}\ M_\odot\ yr^{-1}$. Given the uncertainties involved, the mass loss derived from optical and radio observations are identical. It would seem that the similar mass transport rates in the HH jet and the CO bullets provide strong support for the view that these CO bullets are not made of ambient material that have been accelerated to these very high velocities, but are mostly composed of material ejected from the central engine (note also the excellent agreement in velocities at optical and radio wavelengths—see above).

Can the HH jet drive the observed molecular outflow?—The above-mentioned mass-loss rate of $4.0 \times 10^{-7}\ M_\odot\ yr^{-1}$ corresponds to a momentum rate of $1.2 \times 10^{-4}\ M_\odot\ yr^{-1}$ km s^{-1}, assuming a velocity for the material of 300 km s^{-1} (note, however, that some of the bullets associated to bow shock *P* and optical knots *Q*, *R*, and *S* are moving at velocities as large as 500 km s^{-1} and that the mass loss inferred from the actual inner molecular jet is also higher). The momentum in the molecular gas at intermediate velocities is about $1.0\ M_\odot\ yr^{-1}$ km s^{-1}. If the jet momentum were transfered to the ambient gas with 100% efficiency, the jet would have to maintain *on average* the same level of activity for 8×10^3 yr. In this time, the VLA source would have roughly 20 ejections of matter, if the frequency is one every 500 yr. The actual momentum in each bullet is typically $0.05\ M_\odot$ km s^{-1}. The fact that the outermost bullets have very high velocities tells us that the momentum transfer cannot be 100% efficient, and consequently the HH jet could be driving the observed molecular outflow only if the dynamical age of the complex is larger than we derive or if some EHV gas remains undetected. It is worth noting that the actual momentum of the EHV gas in the inner jet could be as high as $0.3\ M_\odot$ km s^{-1} (see bottom panel of Fig. 1) and that new observations by Reipurth, Devine, & Bally (1996) have shown that the HH 111 jet complex is indeed much larger than hitherto thought, so it appears that the HH jet may indeed be able to drive the molecular outflow, even with a much lower momentum transfer efficiency.

We have had useful discussions with Rafael Bachiller, Alex Raga, and Sylvie Cabrit. B. R. thanks Claude Bertout for hospitality at Observatoire de Grenoble, where part of this work was done. This study has been partially supported under CICYT project PB93-048.

REFERENCES

Bachiller, R., & Cernicharo, J. 1990, A&A, 239, 276
Bachiller, R., Cernicharo, J., Martin-Pintado, J., Tafalla, M., & Lazareff, B. 1990, A&A, 231, 174
Cabrit, S., & Bertout, C. 1990, ApJ, 348, 530
Cantó, J., & Raga, A. C. 1991, ApJ, 372, 646
Cernicharo, J. 1991, in The Physics of Star Formation and Early Stellar Evolution, ed. C. Lada & N. Kylafis (NATO ASI Ser.), 287
Cernicharo, J., & Guelin, M. 1987, A&A, 176, 299
Chernin, L. M., & Masson, C. R. 1991, ApJ, 382, L93
Chernin, L., Masson, C., Gouveia dal Pino, E. M., & Benz, W. 1994, ApJ, 426, 204
Gredel, R., & Reipurth, B. 1993, ApJ, 407, L29
———. 1994, A&A, 289, L19
Hartigan, P., Morse, J., & Raymond, J. 1996, in preparation
Heathcote, S., & Reipurth, B. 1992, AJ, 104, 2193
Martín-Pintado, J., & Cernicharo, J. 1987, A&A, 176, L27
Masson, C., & Chernin, L. 1993, ApJ, 414, 230
Morse, J., Heathcote, S., Cecil, G., Hartigan, P., & Raymond, J. 1993, ApJ, 410, 764
Olberg, M., Reipurth, B., & Booth, R. 1992, A&A, 259, 252
Raga, A. C. 1991, AJ, 101, 1472
Raga, A. C., & Cabrit, S. 1993, A&A, 278, 267
Raga, A. C., Cabrit, S., & Cantó, J. 1995, MNRAS, 273, 422
Raga, A. C., Cantó, J., Calvet, N., Rodriguez, L. F., & Torrelles, J. M. 1993, A&A, 276, 539
Reipurth, B. 1989, Nature, 340, 42
Reipurth, B., Devine, D., & Bally, J. 1996, in preparation
Reipurth, B., & Olberg, M. 1991, A&A, 246, 535
Reipurth, B., Raga, A. C., & Heathcote, S. 1992, ApJ, 392, 145
Richer, J. S., Hills, R. E., & Padman, R. 1992, MNRAS, 254, 525
Rodriguez, L. F., & Reipurth, B. 1994, A&A, 281, 882
Stahler, S. W. 1994, ApJ, 422, 616